

DISPLACEMENT-ACCELERATION CONTROL VIA STIFFNESS-DAMPING COLLABORATION

IZURU TAKEWAKI^{*,†}

*Department of Architecture and Architectural Systems, Graduate School of Engineering, Kyoto University, Sakyo, Kyoto
606-8501, Japan*

SUMMARY

An approach is presented to stiffness–damping simultaneous optimization for displacement–acceleration simultaneous control. To make a shear building model stiffer, the sum of mean-square interstorey drifts to stationary random excitations is minimized or the mean-square top-floor absolute acceleration is maximized subject to the constraints on total storey stiffness capacity and total damper capacity. Optimality conditions are derived and a two-step optimization method using the optimality conditions is devised. In the first step, the optimal design is found for a specified set of total storey stiffness capacity and total damper capacity. In the second step, a series of optimal designs is found with respect to a varied set of total storey stiffness capacity and total damper capacity. While increase of total stiffness capacity and increase of total damper capacity are both effective in reduction of deformation, only increase of total damper capacity is effective in reduction of acceleration. Acceleration control is carried out in the second step via increase of total damper capacity. It is shown through numerical examples that the proposed method is efficient and reliable. Copyright © 1999 John Wiley & Sons, Ltd.

KEY WORDS: optimal design; stiffness–damping simultaneous design; passive control; random vibration; displacement–acceleration control; non-proportional damping; design sensitivity analysis

1. INTRODUCTION

The problem treated in the present paper is to find simultaneously the optimal storey stiffness distribution and the optimal passive damper positioning in a shear building model by minimizing the sum of mean-square interstorey drifts of the shear building model to stationary random excitations or by maximizing the mean-square top-floor absolute acceleration from the viewpoint of stiffness design. Since the stiffness distribution and the damping coefficient distribution interact with each other very sensitively, simultaneous optimization of both distributions is often complicated. A new efficient and systematic method is proposed for the *simultaneous optimization* of storey stiffness distributions and damping coefficient distributions. The method is a two-step design method. In the first step, a design is found which satisfies the newly derived optimality conditions for a specified set of total storey stiffness capacity and total damper capacity. In the second step, total storey stiffness capacity and/or total damper capacity are varied with the

* Correspondence to: Izuru Takewaki, Department of Architecture and Architectural Systems, Graduate School of Engineering, Kyoto University, Sakyo, Kyoto 606-8501, Japan

† Associate Professor

optimality conditions satisfied. While deformation is reduced both in the first and second steps, acceleration is reduced only in the second step via increase of total damper capacity. It is also shown numerically that deformation minimization and acceleration maximization are almost equivalent. The features of the present formulation are to deal with any damping system, e.g. proportional or non-proportional, Voigt type or Maxwell type, to treat any structural system so far as it can be modelled with finite element systems, to treat any random excitations (any configuration of spectral density functions) if stationary and to consist of a systematic algorithm without any indefinite iterative operation.

While research on active and passive control has been developed extensively (see, for example, References 1–3, research on optimal passive damper positioning has been limited. Especially research on simultaneous optimization of stiffness and damping is very limited. The following studies may be relevant to the present paper. Gurgoze and Muller⁴ presented a numerical method for finding the optimal placement and the optimal damping coefficient for a single viscous damper in a prescribed linear multi-degree-of-freedom system. Hahn and Sathiyaveeswara⁵ performed several parametric studies on the effects of damper distribution on the earthquake response of shear buildings, and showed that, for a building with uniform storey stiffnesses, dampers should be added to the lower half floors of the building. Zhang and Soong⁶ proposed a sophisticated seismic design method to find the optimal configuration of viscous dampers for a building with specified storey stiffnesses. In spite of a heuristic criterion that an additional damper should be placed sequentially on the storey with the maximum interstorey drift, it is simple, efficient and pioneering. Tsuji and Nakamura⁷ proposed an algorithm to find both the optimal storey stiffness distribution and the optimal damper distribution for a shear building model subjected to a set of spectrum-compatible earthquakes. The approach by Tsuji and Nakamura⁷ is interesting, but it requires much computational effort and their problem includes artificial constraints, i.e. upper bounds of damping coefficients. Masri *et al.*⁸ presented a simple yet efficient optimum active control method for reducing the oscillations of distributed parameter systems subjected to arbitrary deterministic or stochastic excitations. While they deal with active control, the result is informative to the development in passive optimal control theories. Takewaki *et al.*^{9–12} proposed a new method, called a steepest direction search method, of optimal damper placement for structures with *given stiffnesses*.

2. PROBLEM OF STIFFNESS–DAMPING SIMULTANEOUS OPTIMIZATION FOR MINIMUM DEFORMATION OR MAXIMUM ACCELERATION: ILLUSTRATIVE EXAMPLE

Consider a two-storey damped shear building model as shown in Figure 1. It is assumed here that structural damping is negligible compared with added viscous damping. Let $\{m_1, m_2\}$, $\{k_1, k_2\}$, $\{c_1, c_2\}$ denote floor masses, storey stiffnesses and storey damping coefficients. Assume that $\{m_1, m_2\}$ are prescribed. The design variables are $\{k_1, k_2\}$ and $\{c_1, c_2\}$. Let u_1 and u_2 denote the displacements of masses m_1 and m_2 , respectively. When this model is subjected to a stationary random base acceleration \ddot{u}_g with zero mean, the equation of motion for this model can be written as

$$\begin{bmatrix} k_1 + k_2 & -k_2 \\ -k_2 & k_2 \end{bmatrix} \begin{Bmatrix} u_1 \\ u_2 \end{Bmatrix} + \begin{bmatrix} c_1 + c_2 & -c_2 \\ -c_2 & c_2 \end{bmatrix} \begin{Bmatrix} \dot{u}_1 \\ \dot{u}_2 \end{Bmatrix} + \begin{bmatrix} m_1 & 0 \\ 0 & m_2 \end{bmatrix} \begin{Bmatrix} \ddot{u}_1 \\ \ddot{u}_2 \end{Bmatrix} = - \begin{bmatrix} m_1 & 0 \\ 0 & m_2 \end{bmatrix} \begin{Bmatrix} 1 \\ 1 \end{Bmatrix} \ddot{u}_g \quad (1)$$

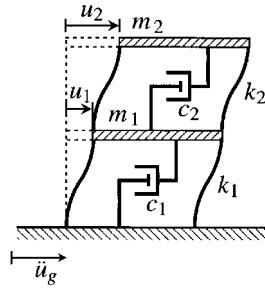


Figure 1. Two-storey shear building model with added viscous dampers

Let $U_1(\omega)$, $U_2(\omega)$, $\ddot{U}_g(\omega)$ denote the Fourier transforms of u_1 , u_2 , \ddot{u}_g , respectively, and let ω denote a circular frequency. Fourier transformation of equation (1) may be reduced to the following form:

$$\mathbf{A}\mathbf{U}(\omega) = \mathbf{B}\ddot{U}_g(\omega) \quad (2)$$

where

$$\mathbf{A} = \begin{bmatrix} k_1 + k_2 + i\omega(c_1 + c_2) - \omega^2 m_1 & -k_2 - i\omega c_2 \\ -k_2 - i\omega c_2 & k_2 + i\omega c_2 - \omega^2 m_2 \end{bmatrix} \quad (3a)$$

$$\mathbf{B} = - \begin{Bmatrix} m_1 \\ m_2 \end{Bmatrix} \quad (3b)$$

$$\mathbf{U}(\omega) = \begin{Bmatrix} U_1(\omega) \\ U_2(\omega) \end{Bmatrix} \quad (3c)$$

The notation i denotes the imaginary unit.

The Fourier transforms $\Delta_1(\omega)$, $\Delta_2(\omega)$ of the interstorey drifts $d_1 = u_1$, $d_2 = u_2 - u_1$ are related to $U_1(\omega)$, $U_2(\omega)$ by

$$\begin{Bmatrix} \Delta_1(\omega) \\ \Delta_2(\omega) \end{Bmatrix} = \begin{bmatrix} 1 & 0 \\ -1 & 1 \end{bmatrix} \begin{Bmatrix} U_1(\omega) \\ U_2(\omega) \end{Bmatrix} \equiv \mathbf{T}\mathbf{U}(\omega) \quad (4)$$

Let \mathbf{T}_i denote the i th row of the matrix \mathbf{T} . $\Delta_i(\omega)$ may be described as

$$\Delta_i(\omega) = \mathbf{T}_i \mathbf{A}^{-1} \mathbf{B} \ddot{U}_g(\omega) \equiv H_{\Delta_i}(\omega) \ddot{U}_g(\omega) \quad (5)$$

On the other hand, the Fourier transforms $\ddot{\mathbf{U}}(\omega) = \{\ddot{U}_1(\omega) \ \ddot{U}_2(\omega)\}^T$ of the relative floor accelerations \ddot{u}_1 , \ddot{u}_2 are related to $\ddot{U}_g(\omega)$ by

$$\ddot{\mathbf{U}}(\omega) = -\omega^2 \mathbf{U}(\omega) = -\omega^2 \mathbf{A}^{-1} \mathbf{B} \ddot{U}_g(\omega) \quad (6)$$

The Fourier transforms $\ddot{\mathbf{U}}_A(\omega)$ of the floor absolute accelerations are then expressed as

$$\ddot{\mathbf{U}}_A(\omega) = \ddot{\mathbf{U}}(\omega) + \mathbf{1} \ddot{U}_g(\omega) = (\mathbf{1} - \omega^2 \mathbf{A}^{-1} \mathbf{B}) \ddot{U}_g(\omega) \equiv \mathbf{H}_A(\omega) \ddot{U}_g(\omega) \quad (7)$$

where $\mathbf{1} = \{1 \ 1\}^T$.

Let $S_g(\omega)$ denote the power spectral density function of the input $\ddot{u}_g(t)$. Using the random vibration theory, the mean-square response of the i th interstorey drift can be computed from

$$\sigma_{\Delta_i}^2 = \int_{-\infty}^{\infty} |H_{\Delta_i}(\omega)|^2 S_g(\omega) d\omega = \int_{-\infty}^{\infty} H_{\Delta_i}(\omega) H_{\Delta_i}^*(\omega) S_g(\omega) d\omega \quad (8)$$

where $(\)^*$ denotes the complex conjugate. On the other hand, the mean-square response of the i th-floor absolute acceleration may be evaluated by

$$\sigma_{A_i}^2 = \int_{-\infty}^{\infty} |H_{A_i}(\omega)|^2 S_g(\omega) d\omega = \int_{-\infty}^{\infty} H_{A_i}(\omega) H_{A_i}^*(\omega) S_g(\omega) d\omega \quad (9)$$

where $H_{A_i}(\omega)$ is the i th component of $\mathbf{H}_A(\omega)$ defined in equation (7).

The first problem of displacement control may be described as:

Problem D. Find the storey stiffnesses $\{k_1, k_2\}$ and damper damping coefficients $\{c_1, c_2\}$ of the model which minimizes $f = \sum_{i=1}^2 \sigma_{\Delta_i}^2$ subject to $\sum_{i=1}^2 k_i = \bar{W}_K$, $\sum_{i=1}^2 c_i = \bar{W}_C$ and $0 \leq k_i \leq \bar{k}_i$ ($i = 1, 2$), $0 \leq c_i \leq \bar{c}_i$ ($i = 1, 2$) where \bar{W}_K , \bar{W}_C , \bar{k}_i , \bar{c}_i are the prescribed parameters.

The second problem of acceleration control may be stated as:

Problem A. Find the storey stiffnesses $\{k_1, k_2\}$ and damper damping coefficients $\{c_1, c_2\}$ of the model which maximizes $f = \sigma_{A_2}^2$ subject to $\sum_{i=1}^2 k_i = \bar{W}_K$, $\sum_{i=1}^2 c_i = \bar{W}_C$ and $0 \leq k_i \leq \bar{k}_i$ ($i = 1, 2$), $0 \leq c_i \leq \bar{c}_i$ ($i = 1, 2$).

It is well known that, as a structure becomes stiffer, the response acceleration to seismic excitations with wide-band frequency contents becomes larger in general. This property is utilized in Problem A within the context of stiffness design. The correspondence of Problems D and A will be discussed later in numerical examples.

3. PROBLEM OF STIFFNESS-DAMPING SIMULTANEOUS OPTIMIZATION: GENERAL CASE

3.1. Problem

Consider an n -storey damped shear building model subjected to a stationary random horizontal base acceleration \ddot{u}_g with zero mean. The problem of optimal stiffness-damping positioning for displacement-acceleration control may be described as:

Problem SDDA. Find the storey stiffnesses $\mathbf{k} = \{k_i\}$ and damper damping coefficients $\mathbf{c} = \{c_i\}$, which minimize the weighted sum of mean-square interstorey drifts and a mean-square top-floor absolute acceleration

$$f = a \left(\sum_{i=1}^n \sigma_{\Delta_i}^2 \right) + b (D_0 \sigma_{A_n}^2) \quad (10)$$

subject to a constraint on the sum of the storey stiffnesses

$$\sum_{i=1}^n k_i = \bar{W}_K \quad (\bar{W}_K : \text{specified value}) \quad (11a)$$

a constraint on the sum of the damper damping coefficients

$$\sum_{i=1}^n c_i = \bar{W}_C \quad (\bar{W}_C: \text{specified value}) \quad (11b)$$

and to constraints on the storey stiffnesses and damper damping coefficients

$$0 \leq k_i \leq \bar{k}_i \quad (i = 1, \dots, n) \quad (12a)$$

$$0 \leq c_i \leq \bar{c}_i \quad (i = 1, \dots, n) \quad (12b)$$

where \bar{k}_i is the upper bound of the storey stiffness and \bar{c}_i is that of damper damping coefficient. The parameters a, b, D_0 are weighting parameters on deformation and acceleration and a parameter for adjusting dimensions of deformation and acceleration.

Problem D in the previous section corresponds to the parameter set $a = 1, b = 0$ and Problem A corresponds to $a = 0, b = -1$. As shown in the later numerical examples, Problems D and A are almost equivalent. Therefore, the problem with the parameter set of non-zero a and b may not lead to meaningful solutions in the present model. However treatment of objective performances in Problem SDDA is expected to lead to a unified approach for other structural systems. For example, an objective function $f = \sum_{i=2}^n \sigma_{\Delta_i}^2 + D_0 \sum_{i=1}^n \sigma_{A_i}^2$ may lead to generation of base-isolated structures. This subject will be discussed elsewhere. Problems D and A are treated hereafter and Problem SDDA with the parameter set of non-zero a and b is not dealt with directly. Acceleration control is considered in Problem D via increase of total damper capacity. Since the optimality conditions for Problems D, A and SDDA can be derived in a unified manner, its derivation is shown in the following.

The generalized Lagrangian L for Problems D, A and SDDA may be expressed in terms of Lagrange multipliers $\lambda_K, \lambda_C, \boldsymbol{\alpha} = \{\alpha_i\}, \boldsymbol{\beta} = \{\beta_i\}, \boldsymbol{\mu} = \{\mu_i\}, \mathbf{v} = \{v_i\}$.

$$\begin{aligned} L(\mathbf{k}, \mathbf{c}, \lambda_K, \lambda_C, \boldsymbol{\alpha}, \boldsymbol{\beta}, \boldsymbol{\mu}, \mathbf{v}) = & f + \lambda_K \left(\sum_{i=1}^n k_i - \bar{W}_K \right) + \lambda_C \left(\sum_{i=1}^n c_i - \bar{W}_C \right) \\ & + \sum_{i=1}^n \alpha_i (0 - k_i) + \sum_{i=1}^n \beta_i (k_i - \bar{k}_i) + \sum_{i=1}^n \mu_i (0 - c_i) + \sum_{i=1}^n v_i (c_i - \bar{c}_i) \quad (13) \end{aligned}$$

For simplicity of expression, the partial differentiation with respect to design variables is hereafter denoted by $(\)^j \equiv \partial(\) / \partial k_j, (\)_{,j} \equiv \partial(\) / \partial c_j$.

3.2. Optimality criteria

The principal optimality criteria for Problems D, A and SDDA without active upper and lower bound constraints on storey stiffnesses and damping coefficients may be derived from stationarity conditions of $L(\boldsymbol{\alpha} = \boldsymbol{\beta} = \boldsymbol{\mu} = \mathbf{v} = \mathbf{0})$ with respect to $\mathbf{k}, \mathbf{c}, \lambda_K$ and λ_C . The optimality conditions can be described as

$$f^{,j} + \lambda_K = 0 \quad \text{for } 0 < k_j < \bar{k}_j \quad (j = 1, \dots, n) \quad (14a)$$

$$f_{,j} + \lambda_C = 0 \quad \text{for } 0 < c_j < \bar{c}_j \quad (j = 1, \dots, n) \quad (14b)$$

$$\sum_{i=1}^n k_i - \bar{W}_K = 0 \quad (15a)$$

$$\sum_{i=1}^n c_i - \bar{W}_C = 0 \quad (15b)$$

If either of the lower and upper bounds of storey stiffnesses and damper damping coefficients attains its limit, the optimality conditions should be modified to

$$f^{,j} + \lambda_K \geq 0 \quad \text{for } k_j = 0 \quad (16a)$$

$$f^{,j} + \lambda_K \leq 0 \quad \text{for } k_j = \bar{k}_j \quad (16b)$$

$$f_{,j} + \lambda_C \geq 0 \quad \text{for } c_j = 0 \quad (17a)$$

$$f_{,j} + \lambda_C \leq 0 \quad \text{for } c_j = \bar{c}_j \quad (17b)$$

3.3. Solution algorithm

The present method consists of two design stages, i.e. stage (i) and stage (ii) (see Figure 2). In the first stage, an initial model with uniform storey stiffnesses and uniform damping coefficients is introduced for the specified sets of total stiffness capacity and total damping capacity and an optimal design is found at the end of redesign. In the second stage, a series of optimal designs is obtained sequentially for various stiffness and damping capacity levels. It may be convenient to introduce new parameters $s_i = f^{,i+1}/f^{,1}$ and $t_i = f_{,i+1}/f_{,1}$ to express the optimality conditions. The optimality conditions (14a) and (14b) for $0 < k_j < \bar{k}_j$ and $0 < c_j < \bar{c}_j$ for all j can then be described as $s_i = t_i = 1$ ($i = 1, \dots, n-1$).

The linear increments of s_i and t_i may be expressed as

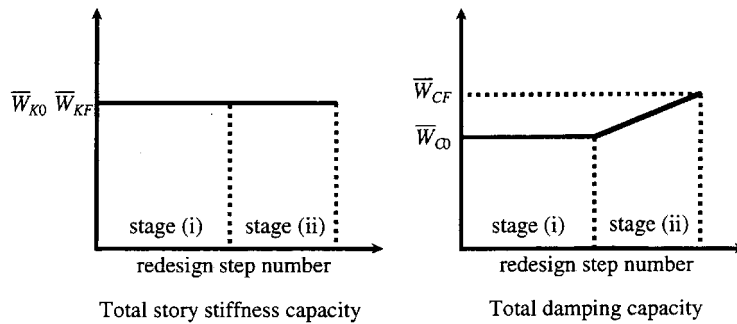
$$\Delta s_i = \frac{1}{f^{,1}} \left(\sum_{j=1}^n f^{,(i+1)j} \Delta k_j + \sum_{j=1}^n f^{,i+1}_{,j} \Delta c_j \right) - \frac{f^{,i+1}}{(f^{,1})^2} \left(\sum_{j=1}^n f^{,1j} \Delta k_j + \sum_{j=1}^n f^{,1}_{,j} \Delta c_j \right) \quad (18a)$$

$$\Delta t_i = \frac{1}{f_{,1}} \left(\sum_{j=1}^n f^{,j}_{,i+1} \Delta k_j + \sum_{j=1}^n f_{,(i+1)j} \Delta c_j \right) - \frac{f_{,i+1}}{(f_{,1})^2} \left(\sum_{j=1}^n f^{,j}_{,1} \Delta k_j + \sum_{j=1}^n f_{,1j} \Delta c_j \right) \quad (18b)$$

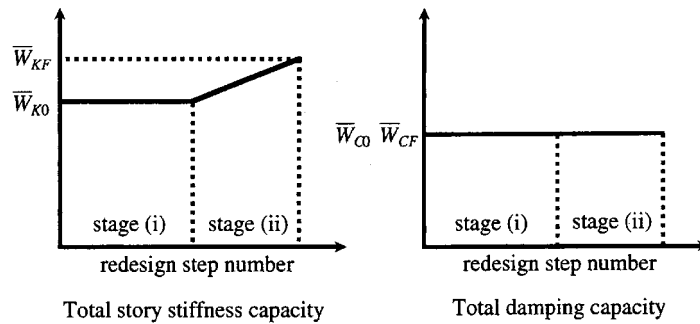
The linear increments of equations (15a) and (15b) can be expressed as

$$\sum_{i=1}^n \Delta k_i - \Delta \bar{W}_K = 0 \quad (19a)$$

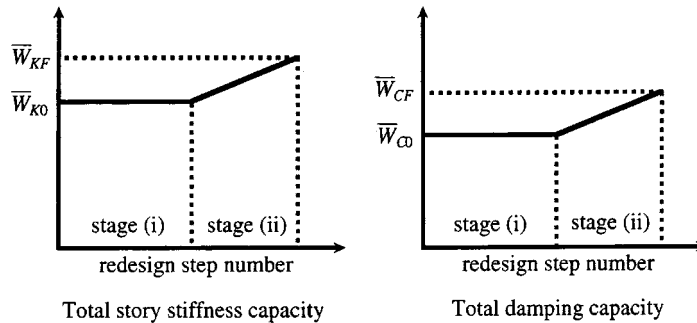
$$\sum_{i=1}^n \Delta c_i - \Delta \bar{W}_C = 0 \quad (19b)$$



Case (1)



Case (2)



Case (3)

Figure 2. Total spring stiffness capacity and total damping capacity in stage (i) and stage (ii)

Note that constraints (11a) and (11b) may be non-linear functions of $\{k_i\}$, $\{c_i\}$ as long as their linear increments can be expressed mathematically. Combination of equation (18) with equation (19) leads to a set of simultaneous linear equations in terms of $\{\Delta k_i\}$, $\{\Delta c_i\}$. An example for

a two-storey model can be expressed as

$$\begin{bmatrix} f_{,1} f_{,21} - f_{,2} f_{,11} & f_{,1} f_{,22} - f_{,2} f_{,12} & f_{,1} f_{,1}^2 - f_{,2} f_{,1}^1 & f_{,1} f_{,2}^2 - f_{,2} f_{,2}^1 \\ 1 & 1 & 0 & 0 \\ f_{,1} f_{,2}^1 - f_{,2} f_{,1}^1 & f_{,1} f_{,2}^2 - f_{,2} f_{,1}^2 & f_{,1} f_{,21} - f_{,2} f_{,11} & f_{,1} f_{,22} - f_{,2} f_{,12} \\ 0 & 0 & 1 & 1 \end{bmatrix} \begin{pmatrix} \Delta k_1 \\ \Delta k_2 \\ \Delta c_1 \\ \Delta c_2 \end{pmatrix} = \begin{pmatrix} \Delta s_1 (f_{,1})^2 \\ \Delta \bar{W}_K \\ \Delta t_1 (f_{,1})^2 \\ \Delta \bar{W}_C \end{pmatrix} \quad (20)$$

In the first stage, the model with uniform storey stiffnesses and uniform damping coefficients is employed as the initial model. The solution algorithm in the case of $k_j < \bar{k}_j$, $c_j < \bar{c}_j$ for all j may be summarized as follows:

Stage (i)

Step 0: Compute initial uniform storey stiffnesses $k_j = \hat{k}$ ($j = 1, \dots, n$) and initial uniform damper damping coefficients $c_j = \hat{c}$ ($j = 1, \dots, n$) for the initial targets \bar{W}_{K0} , \bar{W}_{C0} by $\hat{k} = \bar{W}_{K0}/n$ and $\hat{c} = \bar{W}_{C0}/n$.

Step 1: Calculate $\{s_{0i}\}$, $\{t_{0i}\}$ for the initial model and obtain $\{\Delta s_i\}$, $\{\Delta t_i\}$ by $\Delta s_i = (1 - s_{0i})/N_1$, $\Delta t_i = (1 - t_{0i})/N_1$ where N_1 is the number of redesign steps in stage (i).

Step 2: Find the optimal storey stiffnesses and damper damping coefficients by sequential application of equation (20) with $\Delta \bar{W}_K = 0$, $\Delta \bar{W}_C = 0$.

Stage (ii)

Step 3: Set the targets \bar{W}_{KF} and \bar{W}_{CF} and calculate $\Delta \bar{W}_K$ and $\Delta \bar{W}_C$ by $\Delta \bar{W}_K = (\bar{W}_{KF} - \bar{W}_{K0})/N_2$ and $\Delta \bar{W}_C = (\bar{W}_{CF} - \bar{W}_{C0})/N_2$ where N_2 is the number of redesign steps in stage (ii).

Step 4: Find the optimal storey stiffnesses and damper damping coefficients by sequential application of equation (20) with $\Delta s_i = 0$, $\Delta t_i = 0$ (for all i).

The concept in stage (i) may be somewhat similar to the concept of incremental inverse problems in Reference 13. However in the present problem, optimality criteria are included and higher-order design sensitivities are required. In the present algorithm, the first- and second-order design sensitivities of the objective function are required. These expressions for deformation control may be derived as follows.

First-order sensitivities.

$$(\sigma_{\Delta_i}^2)^{,j} = \int_{-\infty}^{\infty} \{H_{\Delta_i}(\omega)\}^{,j} H_{\Delta_i}^*(\omega) S_g(\omega) d\omega + \int_{-\infty}^{\infty} H_{\Delta_i}(\omega) \{H_{\Delta_i}^*(\omega)\}^{,j} S_g(\omega) d\omega \quad (21a)$$

$$(\sigma_{\Delta_i}^2)^{,j} = \int_{-\infty}^{\infty} \{H_{\Delta_i}(\omega)\}^{,j} H_{\Delta_i}^*(\omega) S_g(\omega) d\omega + \int_{-\infty}^{\infty} H_{\Delta_i}(\omega) \{H_{\Delta_i}^*(\omega)\}^{,j} S_g(\omega) d\omega \quad (21b)$$

Second-order sensitivities.

$$(\sigma_{\Delta_i}^2)^{jl} = \int_{-\infty}^{\infty} \{H_{\Delta_i}(\omega)\}^{,j} \{H_{\Delta_i}^*(\omega)\}^{,l} S_g(\omega) d\omega + \int_{-\infty}^{\infty} \{H_{\Delta_i}(\omega)\}^{,l} \{H_{\Delta_i}^*(\omega)\}^{,j} S_g(\omega) d\omega \\ + \int_{-\infty}^{\infty} \{H_{\Delta_i}(\omega)\}^{,jl} H_{\Delta_i}^*(\omega) S_g(\omega) d\omega + \int_{-\infty}^{\infty} H_{\Delta_i}(\omega) \{H_{\Delta_i}^*(\omega)\}^{,jl} S_g(\omega) d\omega \quad (22a)$$

$$(\sigma_{\Delta_i}^2)^{,j}_l = \int_{-\infty}^{\infty} \{H_{\Delta_i}(\omega)\}^{,j} \{H_{\Delta_i}^*(\omega)\}_{,l} S_g(\omega) d\omega + \int_{-\infty}^{\infty} \{H_{\Delta_i}(\omega)\}_{,l} \{H_{\Delta_i}^*(\omega)\}^{,j} S_g(\omega) d\omega \\ + \int_{-\infty}^{\infty} \{H_{\Delta_i}(\omega)\}_{,l}^j H_{\Delta_i}^*(\omega) S_g(\omega) d\omega + \int_{-\infty}^{\infty} H_{\Delta_i}(\omega) \{H_{\Delta_i}^*(\omega)\}_{,l}^j S_g(\omega) d\omega \quad (22b)$$

$$(\sigma_{\Delta_i}^2)^{,l}_j = \int_{-\infty}^{\infty} \{H_{\Delta_i}(\omega)\}_{,j} \{H_{\Delta_i}^*(\omega)\}^{,l} S_g(\omega) d\omega + \int_{-\infty}^{\infty} \{H_{\Delta_i}(\omega)\}^{,l} \{H_{\Delta_i}^*(\omega)\}_{,j} S_g(\omega) d\omega \\ + \int_{-\infty}^{\infty} \{H_{\Delta_i}(\omega)\}_{,j}^l H_{\Delta_i}^*(\omega) S_g(\omega) d\omega + \int_{-\infty}^{\infty} H_{\Delta_i}(\omega) \{H_{\Delta_i}^*(\omega)\}_{,j}^l S_g(\omega) d\omega \quad (22c)$$

$$(\sigma_{\Delta_i}^2)_{,jl} = \int_{-\infty}^{\infty} \{H_{\Delta_i}(\omega)\}_{,j} \{H_{\Delta_i}^*(\omega)\}_{,l} S_g(\omega) d\omega + \int_{-\infty}^{\infty} \{H_{\Delta_i}(\omega)\}_{,l} \{H_{\Delta_i}^*(\omega)\}_{,j} S_g(\omega) d\omega \\ + \int_{-\infty}^{\infty} \{H_{\Delta_i}(\omega)\}_{,jl} H_{\Delta_i}^*(\omega) S_g(\omega) d\omega + \int_{-\infty}^{\infty} H_{\Delta_i}(\omega) \{H_{\Delta_i}^*(\omega)\}_{,jl} S_g(\omega) d\omega \quad (22d)$$

In equations (21), (22), the sensitivities of transfer functions are expressed as

$$\{H_{\Delta_i}(\omega)\}^{,j} = \mathbf{T}_i(\mathbf{A}^{-1})^{,j} \mathbf{B}, \quad \{H_{\Delta_i}(\omega)\}_{,j} = \mathbf{T}_i(\mathbf{A}^{-1})_{,j} \mathbf{B} \\ \{H_{\Delta_i}(\omega)\}^{,jl} = \mathbf{T}_i(\mathbf{A}^{-1})^{,jl} \mathbf{B}, \quad \{H_{\Delta_i}(\omega)\}_{,l}^j = \mathbf{T}_i(\mathbf{A}^{-1})_{,l}^j \mathbf{B} \\ \{H_{\Delta_i}(\omega)\}_{,j}^l = \mathbf{T}_i(\mathbf{A}^{-1})_{,j}^l \mathbf{B}, \quad \{H_{\Delta_i}(\omega)\}_{,jl} = \mathbf{T}_i(\mathbf{A}^{-1})_{,jl} \mathbf{B} \quad (23a-f)$$

$$\{H_{\Delta_i}^*(\omega)\}^{,j} = \mathbf{T}_i(\mathbf{A}^{-1*})^{,j} \mathbf{B}, \quad \{H_{\Delta_i}^*(\omega)\}_{,j} = \mathbf{T}_i(\mathbf{A}^{-1*})_{,j} \mathbf{B} \\ \{H_{\Delta_i}^*(\omega)\}^{,jl} = \mathbf{T}_i(\mathbf{A}^{-1*})^{,jl} \mathbf{B}, \quad \{H_{\Delta_i}^*(\omega)\}_{,l}^j = \mathbf{T}_i(\mathbf{A}^{-1*})_{,l}^j \mathbf{B} \\ \{H_{\Delta_i}^*(\omega)\}_{,j}^l = \mathbf{T}_i(\mathbf{A}^{-1*})_{,j}^l \mathbf{B}, \quad \{H_{\Delta_i}^*(\omega)\}_{,jl} = \mathbf{T}_i(\mathbf{A}^{-1*})_{,jl} \mathbf{B} \quad (24a-f)$$

Note that operations of complex conjugate and partial differentiation are exchangeable. Furthermore, the first- and second-order sensitivities of \mathbf{A}^{-1} may be described as

$$(\mathbf{A}^{-1})^{,j} = -\mathbf{A}^{-1} \mathbf{A}^{,j} \mathbf{A}^{-1} \quad (25a)$$

$$(\mathbf{A}^{-1})_{,j} = -\mathbf{A}^{-1} \mathbf{A}_{,j} \mathbf{A}^{-1} \quad (25b)$$

$$(\mathbf{A}^{-1})^{,jl} = \mathbf{A}^{-1} (\mathbf{A}^{,l} \mathbf{A}^{-1} \mathbf{A}^{,j} + \mathbf{A}^{,j} \mathbf{A}^{-1} \mathbf{A}^{,l}) \mathbf{A}^{-1} \quad (25c)$$

$$(\mathbf{A}^{-1})_{,l}^j = \mathbf{A}^{-1} (\mathbf{A}_{,l} \mathbf{A}^{-1} \mathbf{A}^{,j} + \mathbf{A}^{,j} \mathbf{A}^{-1} \mathbf{A}_{,l}) \mathbf{A}^{-1} \quad (25d)$$

$$(\mathbf{A}^{-1})_{,j}^l = \mathbf{A}^{-1} (\mathbf{A}^{,l} \mathbf{A}^{-1} \mathbf{A}_{,j} + \mathbf{A}_{,j} \mathbf{A}^{-1} \mathbf{A}^{,l}) \mathbf{A}^{-1} \quad (25e)$$

$$(\mathbf{A}^{-1})_{,jl} = \mathbf{A}^{-1} (\mathbf{A}_{,l} \mathbf{A}^{-1} \mathbf{A}_{,j} + \mathbf{A}_{,j} \mathbf{A}^{-1} \mathbf{A}_{,l}) \mathbf{A}^{-1} \quad (25f)$$

Note that when the sensitivities of $\sigma_{A_i}^2$ are computed, the transfer function $H_{\Delta_i}(\omega)$ must be replaced by $H_{A_i}(\omega)$ defined in equation (7). Furthermore, the sensitivities of the transfer functions $H_{A_i}(\omega)$ must be computed independently of equations (23), (24). As an example, $\{H_{A_i}(\omega)\}^{,j}$ and $\{H_{A_i}(\omega)\}^{,jl}$ can be obtained from $\{H_{A_i}(\omega)\}^{,j} = -\omega^2 \{H_{U_i}(\omega)\}^{,j}$ and $\{H_{A_i}(\omega)\}^{,jl} = -\omega^2 \{H_{U_i}(\omega)\}^{,jl}$ where $\{H_{U_i}(\omega)\}$ is the i th component of $\mathbf{H}_U(\omega) = \mathbf{A}^{-1} \mathbf{B}$.

For a two-storey model, $\mathbf{A}^{,j}$ and $\mathbf{A}_{,j}$ are expressed as

$$\mathbf{A}^{,1} = \begin{bmatrix} 1 & 0 \\ 0 & 0 \end{bmatrix}, \quad \mathbf{A}^{,2} = \begin{bmatrix} 1 & -1 \\ -1 & 1 \end{bmatrix}, \quad \mathbf{A}_{,1} = i\omega \begin{bmatrix} 1 & 0 \\ 0 & 0 \end{bmatrix}, \quad \mathbf{A}_{,2} = i\omega \begin{bmatrix} 1 & -1 \\ -1 & 1 \end{bmatrix} \quad (26)$$

It is interesting to note that, if the matrix \mathbf{A} is a tri-diagonal matrix as in the present model, the inverse of the matrix \mathbf{A} can be expressed in closed form^{12,14} and computational efficiency of the present method is enhanced greatly.

4. NUMERICAL EXAMPLES

Consider a six-storey damped shear building model, as shown in Figure 3, subjected to a stationary band-limited white noise $\ddot{u}_g(t)$ with zero mean whose power spectral density function is given by

$$S_g(\omega) = 0.01(\text{m}^2/\text{s}^3) \quad (-2\pi \times 20 \leq \omega \leq -2\pi \times 0.2, 2\pi \times 0.2 \leq \omega \leq 2\pi \times 20)$$

$$S_g(\omega) = 0 \quad \text{otherwise}$$

For simple presentation of the proposed design method, a rather simple excitation is dealt with. Application of the present method to more general excitations, e.g. one with the Kanai-Tajimi power spectrum or one with the Clough-Penzien power spectrum,¹⁵ is straightforward. Only numerical integration including power spectral density functions has to be modified. The floor masses are prescribed as $m_i = 32.0 \times 10^3$ (kg) ($i = 1, \dots, 6$). The following three examples are presented to demonstrate the practical applicability of the present design method.

Example 1. Deformation minimization

Consider Problem D first. Only the stage (i) is considered in this example. The targets are $\bar{W}_{K0} = 3.38 \times 10^8$ (N/m) and $\bar{W}_{C0} = 7.50 \times 10^6$ (N s/m). The initial uniform storey stiffnesses and uniform dashpot damping coefficients are $k_i = 5.64 \times 10^7$ (N/m) ($i = 1, \dots, 6$) and $c_i = 1.25 \times 10^6$ (N s/m) ($i = 1, \dots, 6$). The number of redesign steps is $N_1 = 100$. Integration in equations (8), (9), (21) and (22) has been made numerically.

Figure 4 shows the plots of storey stiffnesses with respect to the redesign step number. Figure 5 illustrates the variations of dashpot damping coefficients with respect to the redesign step number. It can be observed from Figures 4 and 5 that storey stiffnesses and dashpot damping coefficients exhibit strong non-linearities. Figure 6 shows the variations of parameters $s_i = f^{,i+1}/f^{,1}$ and Figure 7 shows the variations of parameters $t_i = f_{,i+1}/f_{,1}$. It can be seen from Figures 6 and 7 that the optimality conditions $s_i = t_i = 1.0$ for all i are satisfied at the end of the stage (i). Figure 8 illustrates the objective function f (the sum of mean-square interstorey drifts) with respect to the redesign step number. It can be seen that the objective function indeed decreases as the redesign proceeds. Figure 9 shows the mean square of top-floor absolute acceleration with respect to the redesign step number. While the sum of mean squares of

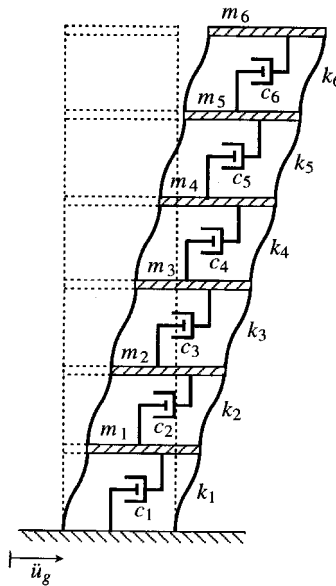


Figure 3. Six-storey shear building model with added viscous dampers

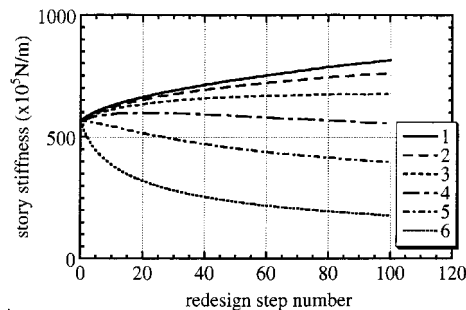


Figure 4. Variation of storey stiffnesses (Example 1)

interstorey drifts decreases, the mean square of top-floor absolute acceleration increases. This means that the shear building model becomes stiffer during this redesign. Undamped fundamental natural period of the model has been shortened from 0.621(s) (initial design) to 0.584(s). The computational errors in this numerical example are within 1.8 (per cent).

Example 2. Acceleration maximization

Consider Problem A. Only stage (i) is considered in this example. The targets are $\bar{W}_{K0} = 3.38 \times 10^8$ (N/m) and $\bar{W}_{C0} = 7.50 \times 10^6$ (N s/m). The initial uniform storey stiffnesses and uniform dashpot damping coefficients are the same as in Example 1. The number of redesign steps is $N_1 = 100$.

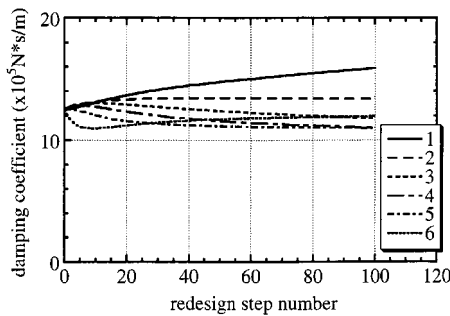


Figure 5. Variation of damper damping coefficients (Example 1)

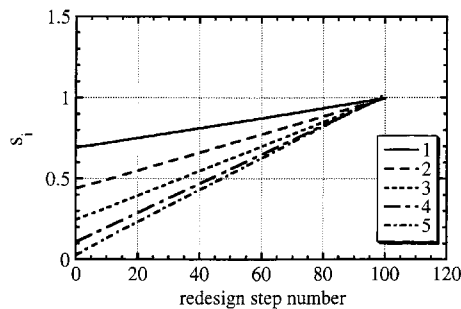
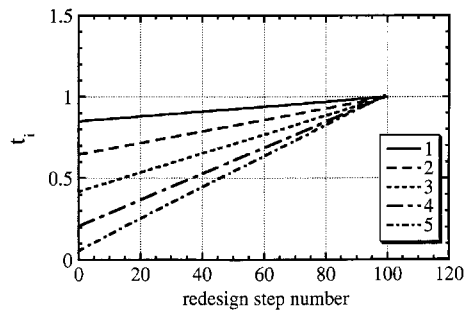
Figure 6. Variation of parameters $s_i = f^{i+1}/f^{i,1}$ (optimality criteria are represented by $s_i = 1$) (Example 1)Figure 7. Variation of parameters $t_i = f_{i+1}/f_{i,1}$ (optimality criteria are represented by $t_i = 1$) (Example 1)

Figure 10 shows the plots of storey stiffnesses with respect to the redesign step number. Figure 11 illustrates the variations of dashpot damping coefficients with respect to the redesign step number. Figure 12 shows the variations of parameters $s_i = f^{i+1}/f^{i,1}$ and Figure 13 shows the variations of parameters $t_i = f_{i+1}/f_{i,1}$. It can be seen from Figures 12 and 13 that the optimality conditions $s_i = t_i = 1.0$ are satisfied at the end of stage (i). Figure 14 illustrates the objective function f (mean square of top-floor absolute acceleration) with respect to the redesign step

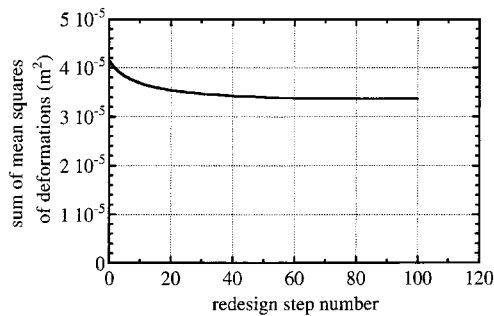


Figure 8. Objective function (sum of mean-square interstorey drifts) with respect to redesign step number (Example 1)

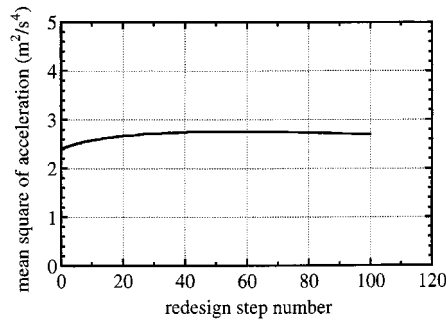


Figure 9. Mean-square top-floor absolute acceleration with respect to redesign step number (Example 1)

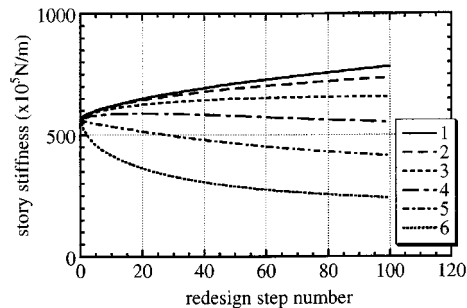


Figure 10. Variation of storey stiffnesses (Example 2)

number. It can be seen that the objective function indeed increases as the redesign proceeds. Figure 15 shows the sum of mean squares of interstorey drifts with respect to the redesign step number. While the mean square of top-floor absolute acceleration increases, the sum of the mean squares of interstorey drifts decreases. This means that the shear building model becomes stiffer also in this redesign. Undamped fundamental natural period of the model has been shortened

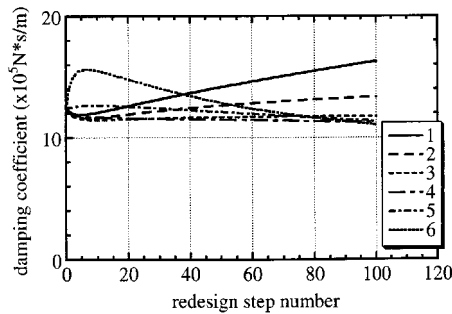
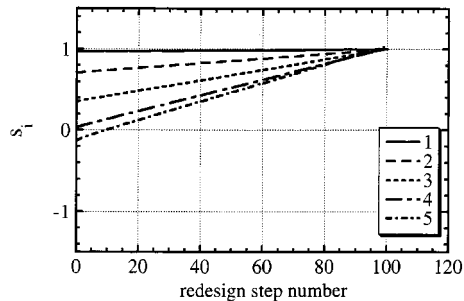
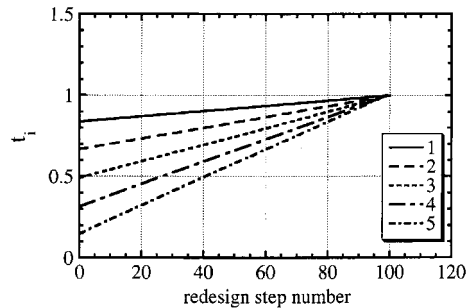


Figure 11. Variation of damper damping coefficients (Example 2)

Figure 12. Variation of parameters $s_i = f^{i+1}/f^1$ (optimality criteria are represented by $s_i = 1$) (Example 2)Figure 13. Variation of parameters $t_i = f_{i+1}/f_1$ (optimality criteria are represented by $t_i = 1$) (Example 2)

from 0.621(s) to 0.583(s). The computational errors in this numerical example are within 3.9 (per cent).

Figure 16 shows the stiffness distributions for Examples 1 and 2. Figure 17 illustrates the damper damping coefficient distributions for Examples 1 and 2. It can be observed that deformation minimization and acceleration maximization are almost equivalent.

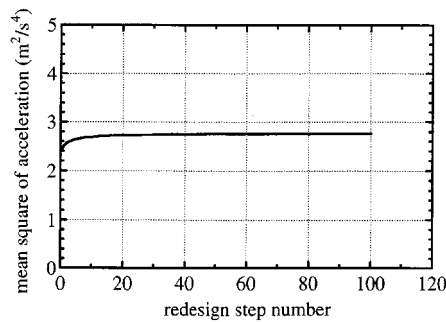


Figure 14. Objective function (mean-square top-floor absolute acceleration) with respect to redesign step number (Example 2)

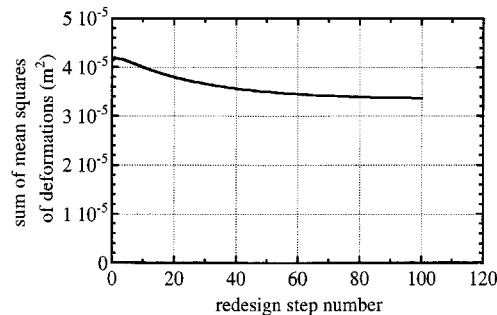


Figure 15. Sum of mean-square interstorey drifts with respect to redesign step number (Example 2)

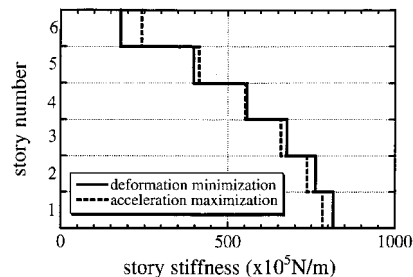


Figure 16. Optimal storey stiffness distributions for minimum deformation and maximum acceleration

Example 3. Two-step design (deformation-acceleration control)

Consider Problem D again. An example for the two-step design method is presented. The sum of mean squares of interstorey drifts has been adopted as the objective function throughout the redesign. Case (1) in Figure 2 has been employed here to reduce the acceleration in stage (ii). The initial targets in stage (i) are $\bar{W}_{K0} = 3.38 \times 10^8$ (N/m) and $\bar{W}_{C0} = 7.50 \times 10^6$ (N s/m). The initial

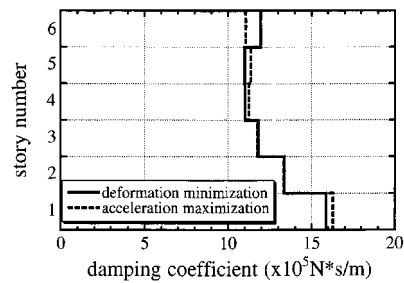


Figure 17. Optimal damping coefficient distributions for minimum deformation and maximum acceleration

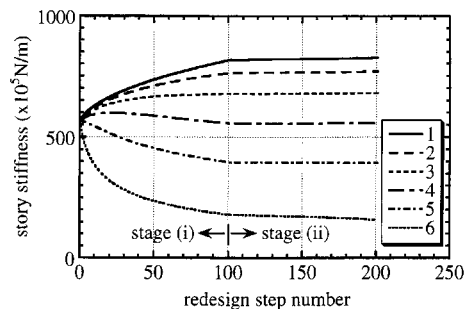


Figure 18. Variation of storey stiffnesses (Example 3)

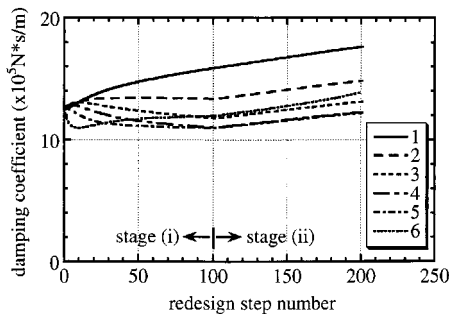


Figure 19. Variation of damper damping coefficients (Example 3)

uniform storey stiffnesses and uniform dashpot damping coefficients are the same as in Examples 1 and 2. The number of redesign steps in the stage (i) is $N_1 = 100$. The final targets in the stage (ii) and $\bar{W}_{KF} = 3.38 \times 10^8 (\text{N/m})$ and $\bar{W}_{CF} = 8.40 \times 10^6 (\text{N s/m})$. The number of redesign steps in the stage (ii) is $N_2 = 100$.

Figure 18 shows the plots of storey stiffnesses with respect to the redesign step number. Figure 19 illustrates the variations of dashpot damping coefficients with respect to the redesign

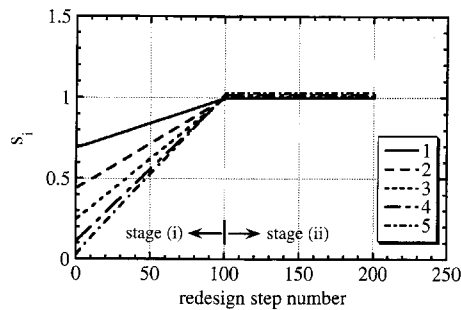


Figure 20. Variation of parameters $s_i = f^{i+1}/f^{i,1}$ (optimality criteria are represented by $s_i = 1$) (Example 3)

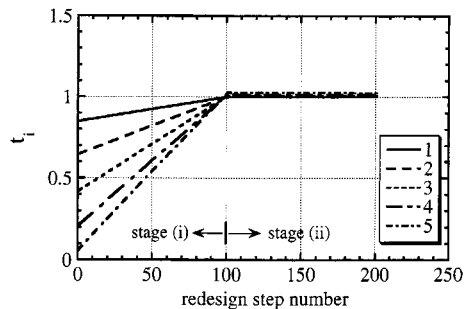


Figure 21. Variation of parameters $t_i = f_{i+1}/f_{i,1}$ (optimality criteria are represented by $t_i = 1$) (Example 3)

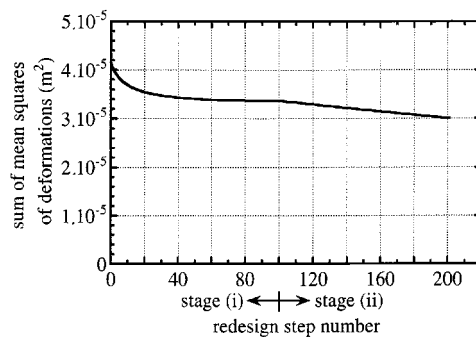


Figure 22. Objective function (sum of mean square interstorey drifts) with respect to redesign step number (Example 3)

step number. It can be observed from Figures 18 and 19 that storey stiffnesses and dashpot damping coefficients exhibit strong non-linearities in stage (i). Figure 20 shows the variations of parameters $s_i = f^{i+1}/f^{i,1}$ and Figure 21 shows the variations of parameters $t_i = f_{i+1}/f_{i,1}$. It can be seen from Figures 20 and 21 that the optimality conditions $s_i = t_i = 1.0$ are satisfied at the end of stage (i) and these conditions *continue to be satisfied* during stage (ii). Figure 22 illustrates the

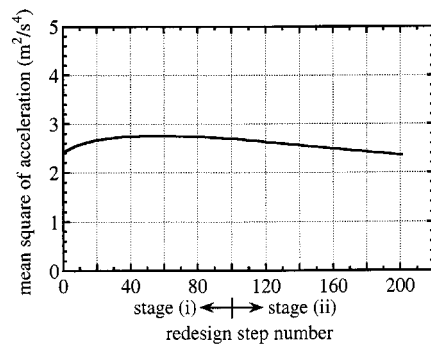


Figure 23. Mean-square top-floor absolute acceleration with respect to redesign step number (Example 3)

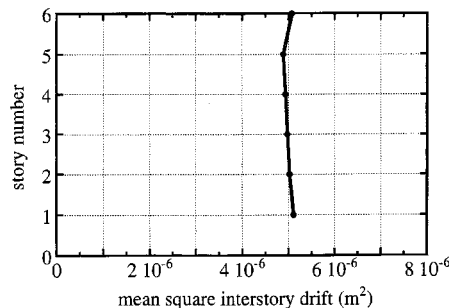


Figure 24. Storey-wise distribution of mean-square interstorey drifts at the end of stage (ii) (Example 3)

objective function f (the sum of mean squares of interstorey drifts) with respect to the redesign step number. Figure 23 shows the mean-square top-floor absolute acceleration with respect to the redesign step number. It can be seen that the objective function (the sum of mean squares of interstorey drifts) indeed decreases as the redesign proceeds and that the mean-square top-floor absolute acceleration decreases in stage (ii) via increase of total damper capacity. From Figure 23 designers can find the target value of total damper capacity satisfying the acceleration constraint. The storeywise distribution of mean-square interstorey drifts of the model at the end of the stage (ii) is shown in Figure 24. It is found that the model at the end of stage (ii) (also in stage (ii)) has an almost uniform distribution of mean-square interstorey drifts. The computational errors in this numerical example are within 1.8 (per cent) in stage (i) and within 1.1 (per cent) in stage (ii).

If the interstorey drift constraints cannot be satisfied only by an increase of total damper capacity, Case (2) or (3) in Figure 2 will have to be utilized as another design path.

5. CONCLUSIONS

A new efficient and systematic procedure has been proposed for simultaneous optimization of storey stiffness distributions and damping coefficient distributions in a shear building model. Due

to high sensitivity of the optimal damping distributions for various stiffness distributions, such simultaneous optimization often causes numerical problems. This problem has been overcome by introducing a design problem to minimize the sum of mean-square deformations to stationary random excitations subject to a constraint on total stiffness capacity and total damping capacity. Another problem has also been posed to maximize the mean-square response of top-floor absolute acceleration subject to the same constraints. The optimal stiffness distribution and the optimal damping coefficient distribution have been determined based upon the newly derived optimality criteria through the concept of incremental inverse problems. It has been shown that deformation minimization and acceleration maximization are almost equivalent and the top-floor absolute acceleration can be reduced effectively by increasing total damper capacity. Efficiency and reliability of the present two-step design procedure have been demonstrated through examples.

The proposed technique is general and is expected to be applicable to other structural systems under non-stationary random excitations. Modified objective functions should then be introduced to express structural performances under non-stationary random excitations.

ACKNOWLEDGEMENT

The present work was partially supported by Grant-in-Aid for Scientific Research (No. 10650562) from the Ministry of Education, Science and Culture of Japan.

REFERENCES

1. G. Housner et al., 'Special issue, structural control: past, present, and future', *J. Engng. Mech. ASCE* **123**(9), 897–971 (1997).
2. T. Kobori, 'Structural control for large earthquakes', *Proc. IUTAM Symp.*, Kyoto, Japan, 1996, pp. 3–28.
3. T. T. Soong and G. F. Dargush, *Passive Energy Dissipation Systems in Structural Engineering*, Wiley, Chichester, 1997.
4. M. Gurgoz and P. C. Muller, 'Optimal positioning of dampers in multi-body systems', *J. Sound Vib.* **158**(3), 517–530 (1992).
5. G. D. Hahn and K. R. Sathiyageeswaran, 'Effects of added-damper distribution on the seismic response of buildings', *Comput. Struct.* **43**(5), 941–950 (1992).
6. R. H. Zhang and T. T. Soong, 'Seismic design of viscoelastic dampers for structural applications', *J. Struct. Engng. ASCE* **118**(5), 1375–1392 (1992).
7. M. Tsuji and T. Nakamura, 'Optimum viscous dampers for stiffness design of shear buildings', *Struct. Des. Tall Buildings* **5**, 217–234 (1996).
8. S. F. Masri, G. A. Bekey and T. K. Caughey, 'Optimum pulse control of flexible structures', *J. Appl. Mech. ASME* **48**, 619–626 (1981).
9. I. Takewaki, 'Optimal damper positioning in beams for minimum dynamic compliance', *Comput. Methods Appl. Mech. Engng* **156**(1–4), 363–373 (1998).
10. I. Takewaki and S. Yoshitomi, 'Effects of support stiffnesses on optimal damper placement for a planar building frame', *Struct. Des. Tall Buildings* **7**(4), 323–336 (1998).
11. I. Takewaki, S. Yoshitomi, K. Uetani and M. Tsuji, 'Non-monotonic optimal damper placement via steepest direction search', *Earthquake Engng. Struct. Dyn.* **28**(6), 655–670 (1999).
12. I. Takewaki and K. Uetani, 'Optimal damper placement for building structures including surface ground amplification', *Proc. 13th ASCE Engineering Mechanics Division Specialty Conf.*, Baltimore, 1999.
13. I. Takewaki, 'Efficient redesign of damped structural systems for target transfer functions', *Comput. Methods Appl. Mech. Engng.* **147**(3/4), 275–286 (1997).
14. I. Takewaki and T. Nakamura, 'Hybrid inverse mode problems for FEM-shear models', *J. Engng. Mech. ASCE* **121**(8), 873–880 (1995).
15. R. W. Clough and J. Penzien, *Dynamics of Structures*, McGraw-Hill, New York, 1975.